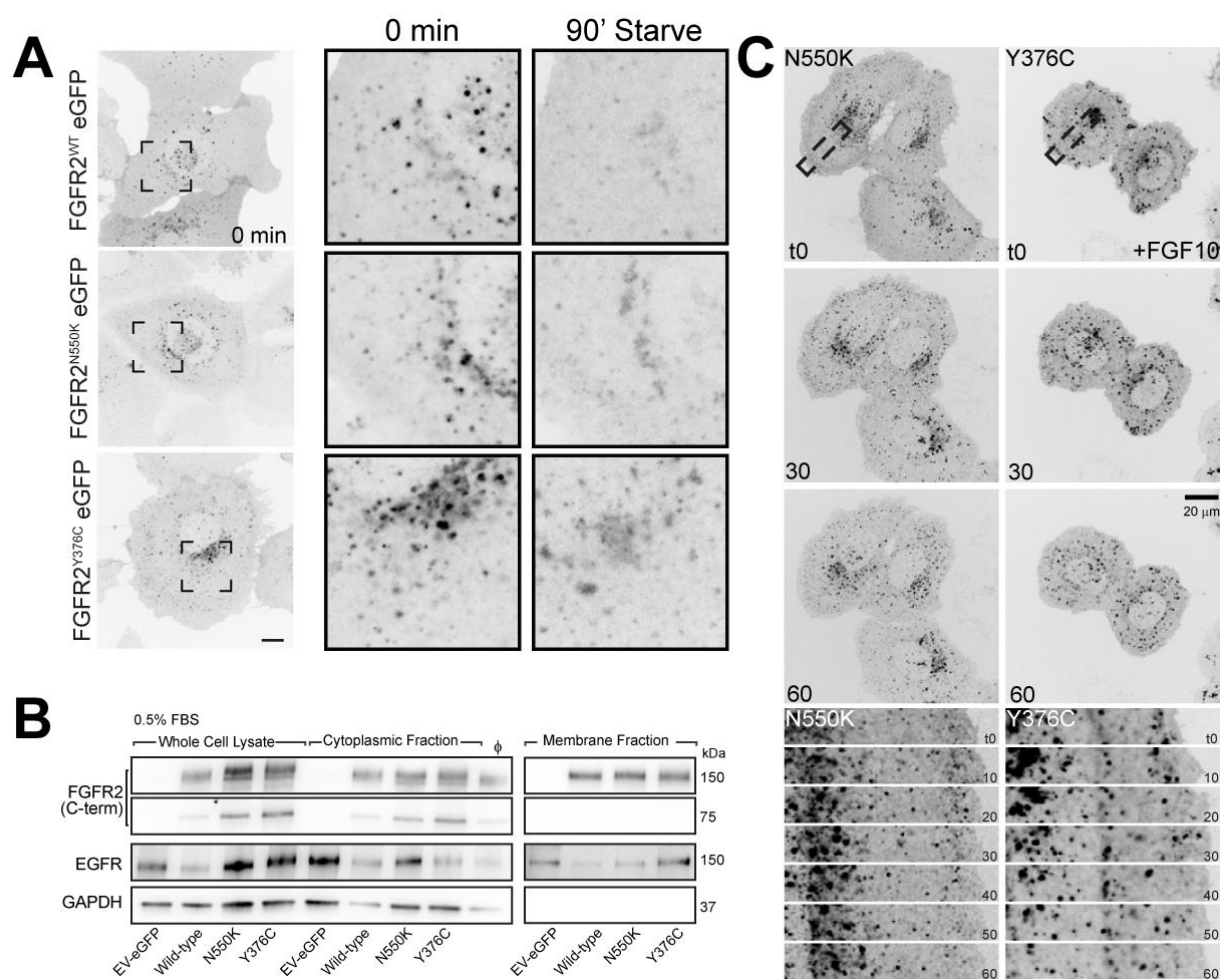


**Supplemental Figure S1. Surface localisation of FGFR2 WT and activating mutants in Ishikawa cells.** (A) Cell intensity surface plots displaying the intensity distribution of pixels of WT, N550K and Y376C expressing cells in 10% FBS. (B) Surface labelling of FGFR2b using an N-terminal FGFR2 antibody in non-permeabilised conditions, 10% FBS. Graph depicting quantitation of surface FGFR integrated fluorescence intensity as a ratio of total eGFP fluorescence. Box-and-whisker plots show median, first and third quartile (box), and 95% confidence intervals (notches) with whiskers extending to the furthest observations within  $\pm 1.5$  times the interquartile range. Dots are individual data points. p-values were calculated by non-parametric Kruskal–Wallis analysis of variance with Dunn's multiple comparisons test correction and are displayed on graph. (C) FGFR2 activating mutant receptors are not on the cell surface in baseline conditions (10% FBS). Cells surface proteins were labelled with Biotin then immunoprecipitated with streptavidin magnetic beads overnight at 4°C (lanes labelled 'Membrane'). Levels of FGFR2 and cadherin were analysed by Western blot. Cadherin was used as a loading control for cell surface proteins (membrane/biotinylated fraction). GAPDH was used as a loading control for non-biotinylated whole cell extracts (WCL) and cytoplasmic fractions. (D) Biological replicates of immunoblot of FGFR2 WT and N550K, Y376C mutant cell lines in normal growth conditions (10% FBS) probed for FGFR2 and activated pathways. Tubulin was used as a loading control. (E) Densitometry analysis of pPLC $\gamma$ , pFRS2 $\alpha$  and pFGFR signalling in 10% FBS. Graphs are three-independent biological replicates. Graphs display mean  $\pm$  SEM. (F) Receptor dimerization of Y376C FGFR2b mutant in the presence and absence of FGF10 ligand, indicated by bands at 260KDa. + marks samples treated with FGF10 and heparin. Samples were lysed in iodoacetamide to prevent disulphide bond formation after lysis, and subjected to gel electrophoresis under non-reducing conditions.

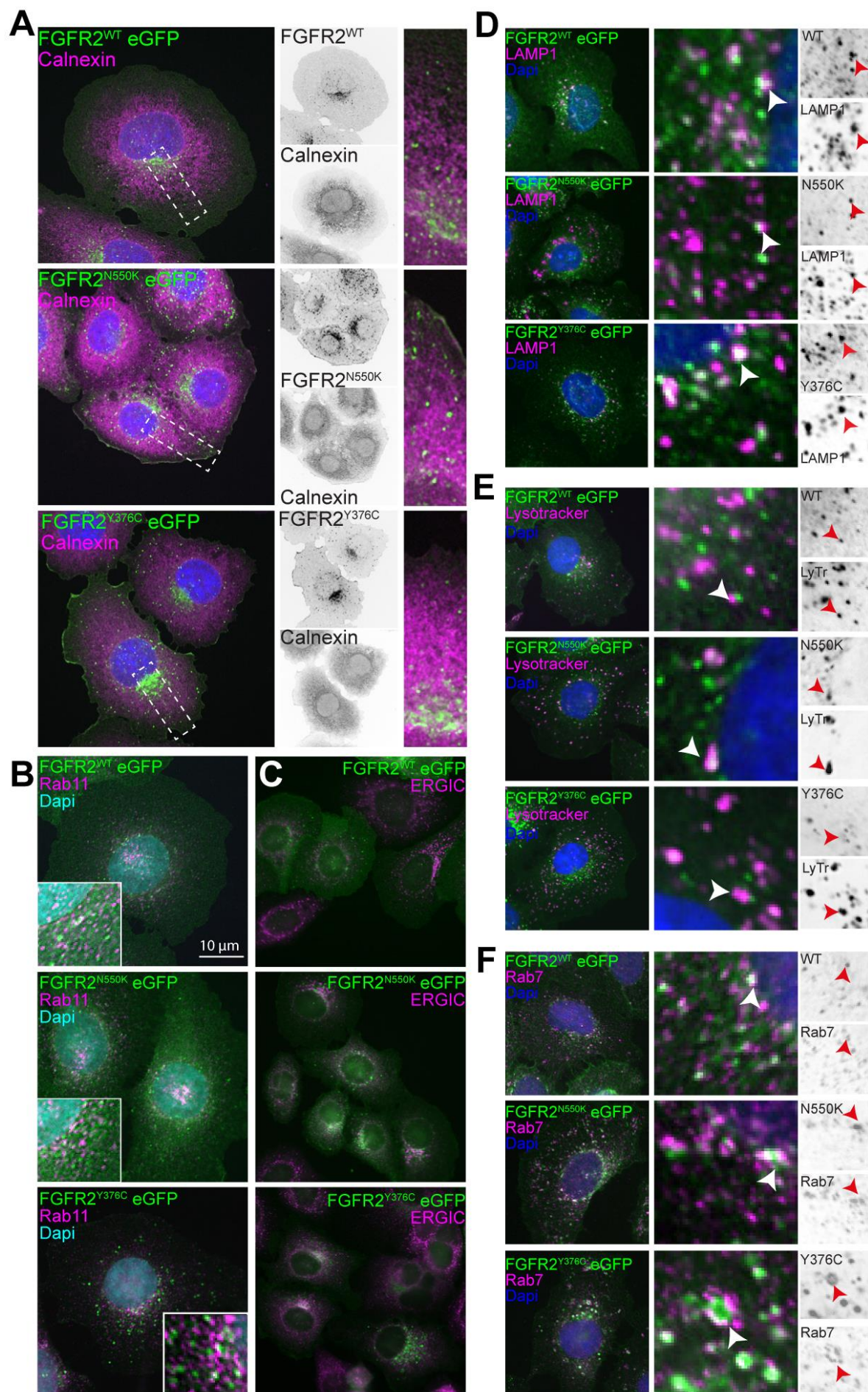


### Supplemental Figure S2. Activating FGFR2 mutants are recruited to the surface in

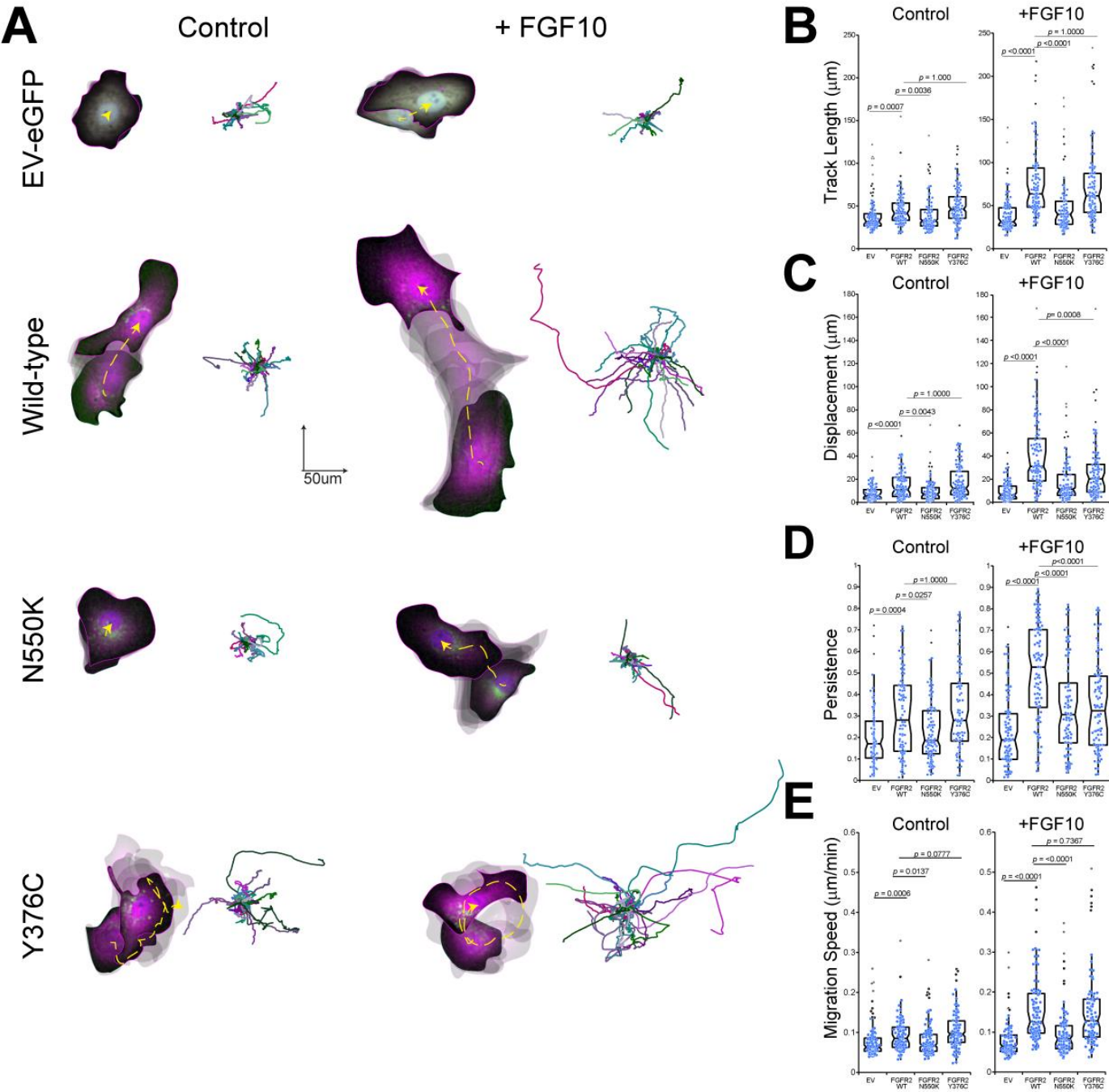
**serum-starved conditions and internalize in response to ligand in Ishikawa cells (A)**

Live-cell spinning disc confocal microscopy of Ishikawa cells stably expressing FGFR2 WT, Y376C or N550K-eGFP, at baseline (0 min) and serum starved (90 min; 0.5% FBS). Insets are magnified intracellular regions outlined by boxed regions. The intracellular pool of receptor decreases suggesting surface recruitment. (B) FGFR mutant receptors are recruited to the surface in serum starved conditions. Cells were starved for 2 hours in 0.5% serum prior to surface biotinylation. Cells surface proteins were labelled with Biotin then immunoprecipitated with streptavidin magnetic beads overnight at 4°C (membrane fraction). Levels of FGFR2 and EGFR were analysed by Western blot. EGFR was used as a loading control for cell surface proteins (membrane fraction). GAPDH was used as a loading control for non-biotinylated whole cell extracts (WCL) and cytoplasmic fractions. (C) Mutant FGFR2 receptors recruited to the surface by serum-starvation internalise in response to FGF10 ligand. Timelapse images of cells expressing N550K or Y376C, serum starved (0.5% FBS 2h) and stimulated with FGF10 (60 minutes). Magnified regions outlined in t0, in 10 minute intervals. Single colour images are inverted for contrast.



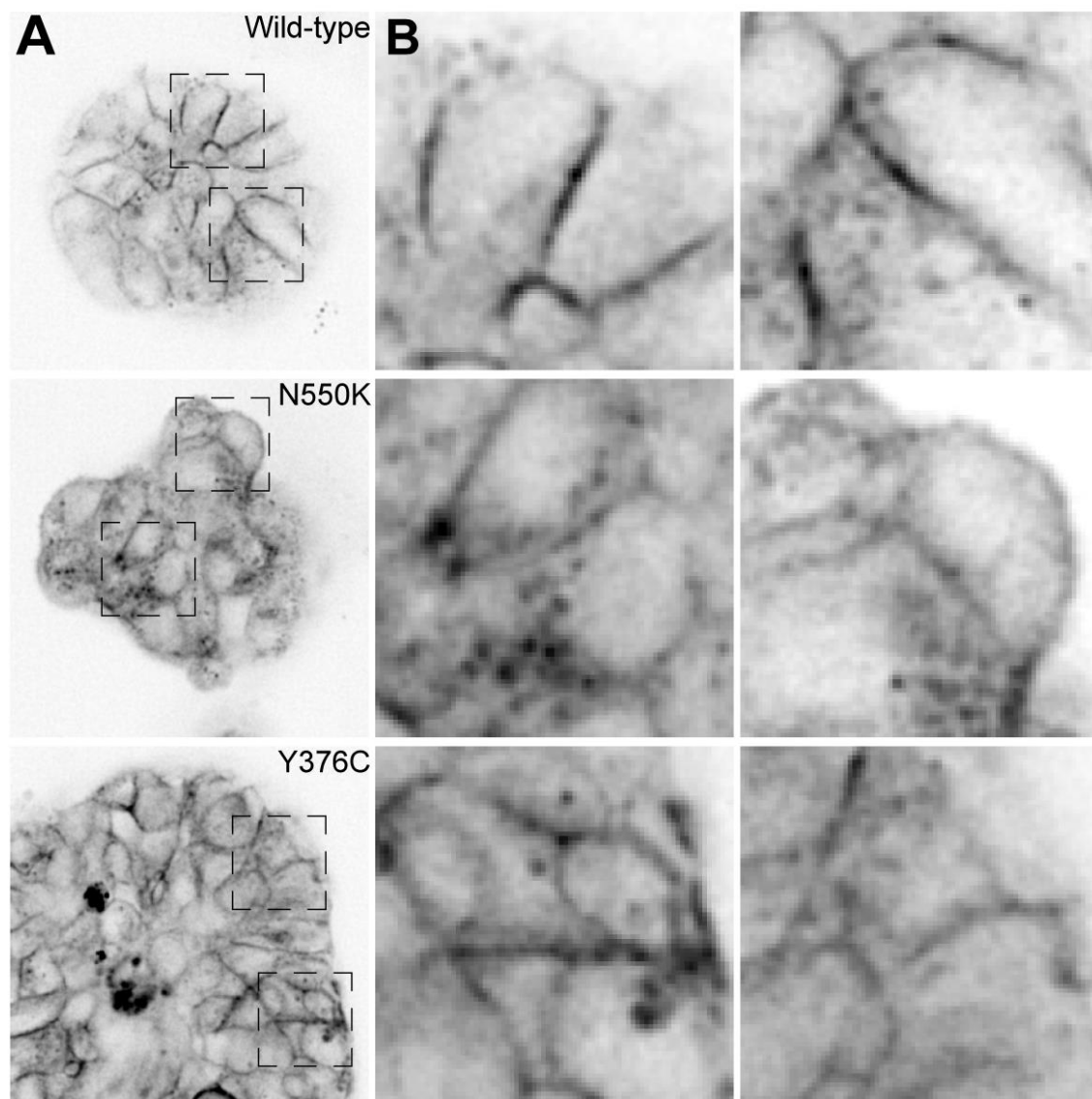


**Supplemental Figure S3. Localisation of intracellular FGFR WT and mutant receptor pools.** Immunofluorescence of the endoplasmic reticulum, ER-Golgi and recycling and late-endosomal compartments in Ishikawa cells expressing FGFR2-WT or activating mutants. Representative images of FGFR2 WT, N550K and Y376C-eGFP expressing cells fixed and stained for; (A) calnexin (magenta) to identify the endoplasmic reticulum, (B) the recycling endosome marker Rab11 (magenta), (C) the ER-Golgi marker ERGIC (magenta) (D) the lysosome markers LAMP1 (magenta), (E) LysoTracker (magenta), (F) or the late endosome marker Rab7 (magenta). Arrowheads identify compartments which overlap with FGFR-eGFP positive structures. Images in **A** are spinning disc confocal images, images in **B-F** are epifluorescent images. DAPI is used as a nuclear stain. Single colour images are inverted for contrast in A, D-F.





**Supplemental Figure S4. FGFR mutant cells do not migrate persistently during FGF-induced chemokinesis.** (A) Spinning disc confocal time lapse sequence of cells co-expressing mCherry (magenta) with empty-vector (EV-eGFP), eGFP-tagged Wild-type FGFR, or mutant (N550K, Y376C) (green), stimulated with heparin alone (5  $\mu$ g/ml, control) or heparin plus FGF10 (50 ng/ml), Hoechst 33342 was used to identify cell nuclei (blue). Cell outlines displayed are traces outlined every 50 minutes for 8 hours. The initial frame (T0) is outlined in green and the final frame (Tfinal) is outlined in magenta, remaining time points are opaque. Cell migration paths are outlined in yellow (dotted line). Plots of representative cell migration paths in control (Heparin) and FGF-treated cells (50 ng/ml). The 30 longest paths from each condition are displayed. Cells were tracked in Imaris (Bitplane) using the “ImarisTrack” function using the analysis criteria outlined in methods. Migration paths were normalized to the starting position. Representative data set of three independent experiments. Analysis of cell migration from three experiments, n= 90 cells per condition; Analysis of cell migration from three experiments; (B) Total track length ( $\mu$ m), (C) Cell displacement (shortest distance between T0 and Tfinal;  $\mu$ m), (D) Persistence index (ratio of cell displacement to total track length), (E) cell migration speed ( $\mu$ m/s). The box-and-whisker plots show median, first and third quartiles (boxes) and 95% confidence intervals (notches) with whiskers extending to the furthest observations within +/- 1.5 times the interquartile range. Dots are individual data points. *p*-values were calculated by non-parametric Kruskal–Wallis analysis of variance with Bonferroni error correction.



**Supplemental Figure S5. Comparison of FGFR mutant localisation in 3-Dimensional endometrial acini.** (A) Representative 2 µm spinning disc confocal optical apical sections of Ishikawa acini grown in growth factor reduced Matrigel™ overlay assay. Ishikawa cells expressing eGFP-tagged Wild-type FGFR, or mutant (N550K, Y376C) (green) grown for 8 days to form acini. (B) Magnified intracellular regions from **A**.



Primary antibodies	Species	Source (Catalog and clone number)	Research Resou	Dilution (for immunoblotting)
FGFR2 (C-17) SC	rabbit	Santa Cruz Technologies (Bek antibody sc-122, C-17)	AB_631509	1:500 (n/a)
Bek H80	rabbit	Santa Cruz Technologies (Bek antibody sc-20735, H-80)	AB_2103394	1:500 (n/a)
β4 integrin	mouse	Millipore (MAB 1964)	AB_2129155	1:100 (1:1000)
GFP	rabbit	Cell Signaling Technology (2956)	AB_1196615	1:200 (1:500)
PLCy	rabbit	Cell Signaling Technology (5690)	AB_10691363	n/a (1:1000)
PLCy/T783	rabbit	Cell Signaling Technology (2821)	AB_2163703	n/a (1:1000)
pFRS2a	rabbit	Cell Signaling Technology (3861)	AB_2231950	n/a (1:1000)
FRS2a	mouse	Santa Cruz Technologies (Bek antibody sc-17841, A-5)	AB_2106230	n/a (1:500)
4370	mouse	Cell Signaling Technology (4370)	AB_2315112	n/a (1:2000)
ERK 1/2	mouse	Santa Cruz Technologies (sc-514302, C-9)	AB_2571739	n/a (1:5000)
AKT (pan)	mouse	Cell Signaling Technology (2920)	AB_1147620	n/a (1:1000)
AKT pS473	rabbit	Cell Signaling Technology (4060)	AB_2315049	n/a (1:1000)
pGFR	rabbit	Cell Signaling Technology (3471)	AB_331072	n/a (1:1000)
pan-cadherin	rabbit	Cell Signaling Technology (4073)	AB_10695251	n/a (1:1000)
EGFR	rabbit	Cell Signaling Technology (4267)	AB_2246311	n/a (1:1000)
α-tubulin	mouse	Sigma (T9026, DM1A)	AB_477593	n/a (1:10000)
Calnexin	rabbit	Abcam (ab75801)	AB_1310022	1:200 (n/a)
GM130	mouse	BD Transduction Laboratories (610822, 35/GM130)	AB_398141	1:1000 (n/a)
ERGIC-53	mouse	Enzo Life Sciences (ALX-804-602-C100)	AB_2051363	1:200 (n/a)
LAMP1	rabbit	Abcam (ab24170)	AB_775978	1:1000 (n/a)
Rab7	rabbit	Cell Signaling Technology (9367)	AB_1904103	1:500 (n/a)

Highly cross absorbed secondary antibodies for immunofluorescence	Source (Catalog number)	Dilution
Alexa488 donkey anti-rabbit	Jackson Immuno Research (711-545-152)	AB_2340684 1:500
TRITC donkey anti-mouse	Jackson Immuno Research (715-025-151)	AB_2340767 1:500

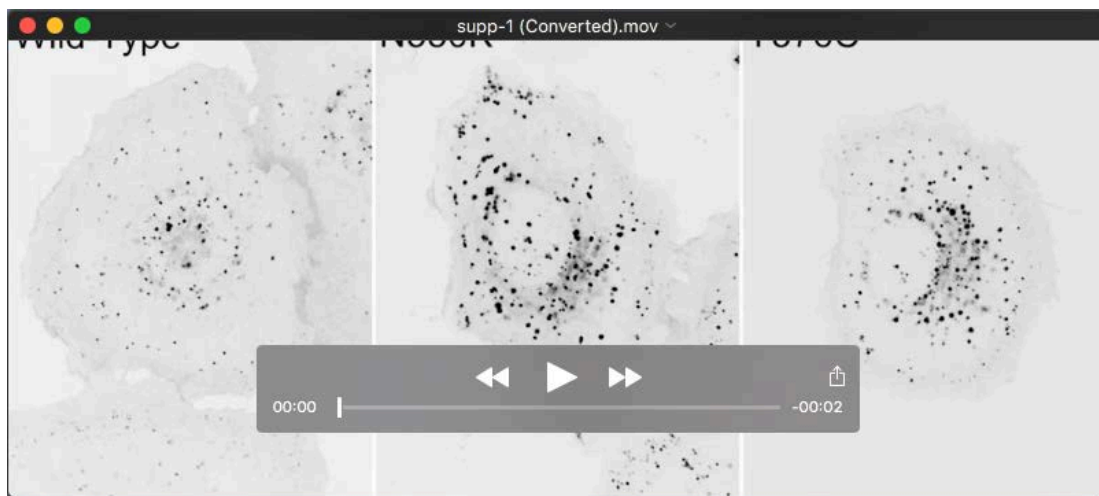
Other reagents for immunofluorescence	Source (Catalog number)	Dilution
Rhodamine Phalloidin	Invitrogen (A12379)	AB_2315147 1:500
Alexa488 phalloidin	Invitrogen (A12379)	AB_2315147 1:500
Hoescht 33342	Molecular Probes (H13991)	no ID available 1:5000
DAPI	Invitrogen (D3571)	AB_2307445 1:10000
Lysotracker	Invitrogen (L7528)	no ID available 2 μM

**Supplemental Table 1. List of Antibodies and Dyes.** Primary antibodies used for immunofluorescence and immunoblotting including specific dilutions.

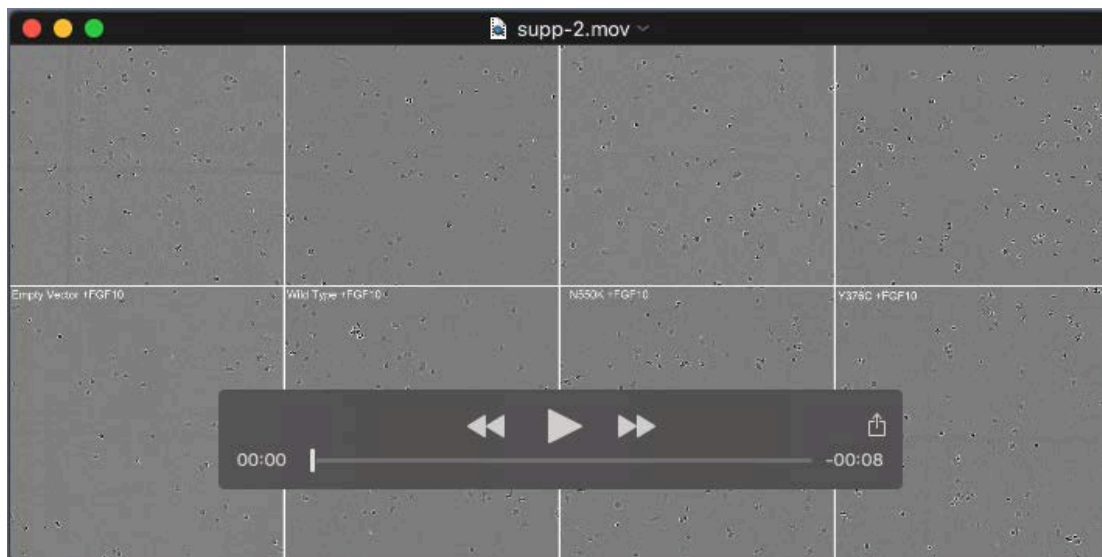
Figure	Statistical test used	S.D or S.E.M	n-values and definition	# of times experiment was replicated in laboratory	P value
<b>1B Vesicle size</b>	one way ANOVA, Kruskal Wallis	Box and whiskers, min and max  Mean $\pm$ SD WT 0.422 $\pm$ 0.08, N550K 0.62 $\pm$ 0.12, Y376C 0.525 $\pm$ 0.15,	per cell (n). 23 (WT), 20 (N550K) 20 (Y376C)	Two independent biological replicates	WT vs. N550K <0.0001 Y376C 0.0177  P values displayed on graph
<b>1B Vesicle number</b>	one way ANOVA, Kruskal Wallis	Box and whiskers, min and max  Mean $\pm$ SD WT 107.4 $\pm$ 59 N550K 165.7 $\pm$ 88, Y376C 133 $\pm$ 126	per cell (n). 23 (WT), 20 (N550K) 20 (Y376C)	Two independent biological replicates	WT vs. N550K 0.0256 Y376C >0.9999  P values displayed on graph
<b>Figure 1D MSD</b>	Dotted line is mean, solid line is a linear trend line fitted to the average vesicle trajectories (dotted line)	n/a	n = vesicles 225 (WT) 93 (N550K) 182 (Y376C)	Pooled from 3 cells, imaged on two independent days	n/a
<b>Figure 1F TIRF</b>	one way ANOVA, Kruskal Wallis	Box and whiskers, min and max  Mean $\pm$ SD WT 5859 $\pm$ 2832, N550K 3099 $\pm$ 1028, Y376C 2695 $\pm$ 839	Per ROI, 7-9 per cell n = ROI 48 (WT) 74 (N550K) 54 (Y376C)	Two independent biological replicates	WT vs. N550K <0.0001 Y376C <0.0001
<b>Supp Fig 2B Surface labelling</b>	one way ANOVA, Kruskal Wallis	Box and whiskers, min and max Mean $\pm$ SD WT 0.40 $\pm$ 0.064 N550K 0.312 $\pm$ 0.128, Y376C 0.233 $\pm$ 0.0732	n = cell 32 (WT) 40 (N550K) 29 (Y376C)	Two independent biological replicates	WT vs. N550K 0.0006 Y376C <0.0001
<b>Figure 2D Internalisation</b>	Solid line is mean	95% confidence interval (dashed lines)	n = cell 11 (WT) 13 (N550K) 11 (Y376C)	Two independent biological replicates	n/a
<b>Figure 2G SRB</b>	One way ANOVA Kruskal-Wallis	Mean $\pm$ SD EV 1 $\pm$ 0.112 EV FGF 1.04 $\pm$ 0.105 WT 1.20 $\pm$ 0.098 WT +FGF 1.26 $\pm$ 0.077 N550K 1 $\pm$ 0.109 N550K +FGF 0.55 $\pm$ 0.040 Y376C 0.78 $\pm$ 0.068 Y376C +FGF 1.04 $\pm$ 0.090	n= well 6 (all conditions)	3 technical triplicates performed on two independent occasions	P values displayed on graph
<b>Figure 4B Golgi Angle</b>	One way ANOVA Kruskal-Wallis	95% confidence interval (notches in box plot)	n = cell 149 (EV), 121 (WT), 227 (N550K), 189 (Y376C).	Three independent biological replicates	WT vs Ev 0.0287 N550K <0.0001 Y376C <0.0001
<b>Figure 4D Wound closure rate</b>	One way ANOVA Kruskal-Wallis	Box-and-whisker plots show median, first and third quartile (box), and 95% confidence intervals (notches) with whiskers extending to the furthest observations within $\pm$ 1.5 times the interquartile range	n = wound condition n = 12	Three independent experiments with n = 4 biological replicates per condition/experiment.	WT vs EV 0.86 N550K 0.05 Y376C 0.002  WT FGF10 vs EV FGF10 <0.001 N550K FGF10 <0.001 Y376C FGF10 0.001
<b>Figure 5B-E Chemotaxis</b>	One way ANOVA Kruskal-Wallis	Box and whiskers, min and max 95% confidence interval (notches in box plot)	n = cell 90 (WT) 90 (N550K) 90 (Y376C)	Three independent biological replicates	P values displayed on graph
<b>Supplementary Figure 4B-E Chemokinesis</b>	One way ANOVA Kruskal-Wallis	Box and whiskers, min and max 95% confidence interval (notches in box plot)	n = cell 90 (WT) 90 (N550K) 90 (Y376C)	Three independent biological replicates	P values displayed on graph
<b>Figure 6D Acini size</b>	One way ANOVA Kruskal-Wallis	Box and whiskers, min and max  Mean $\pm$ SD EV 3343 $\pm$ 1320 WT 3447 $\pm$ 0.1673 N550K 5901 $\pm$ 3123, Y376C 9217 $\pm$ 4235	n = acini 27 (EV) 33 (WT) 28 (N550K) 38 (Y376C)	Three independent biological replicates	WT vs Ev >0.9999 N550K 0.0062 Y376C <0.0001
<b>Figure 6E Acini morphology</b>	n/a	S.E.M	n = acini 87 (EV) 92 (EV +FGF10) 73 (WT) 69 (WT+ FGF10) 83 (N550K) 66 (N550K+FGF10) 83 (Y376C) 75 (Y376C +FGF10)	Three independent biological replicates	n/a

Supplemental Table S2. Complete statistical summary analysis.

## SUPPLEMENTAL VIDEOS

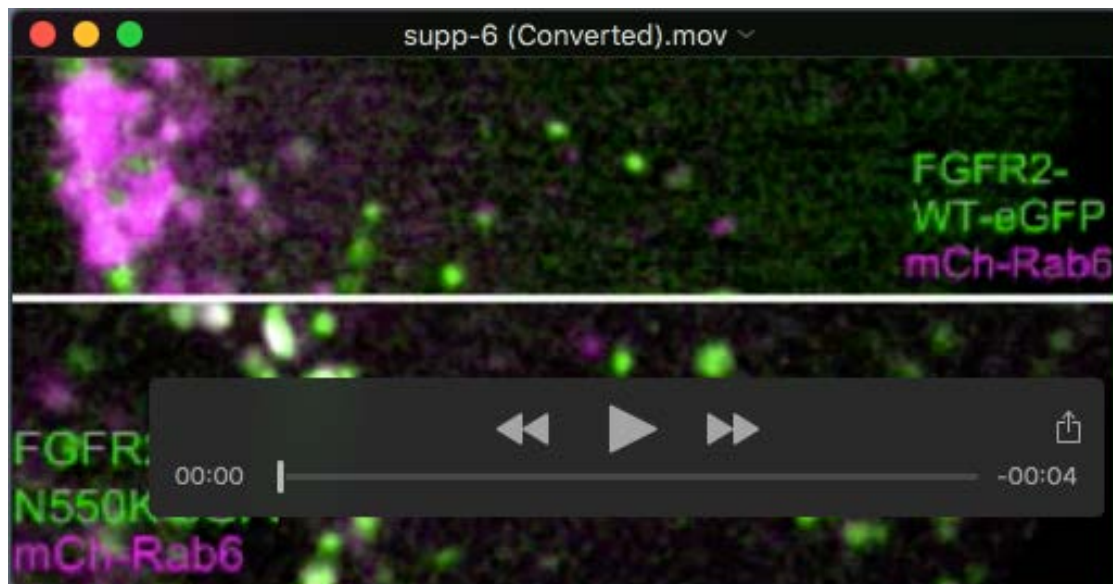


**Supplemental Movie 1.** Dynamics of eGFP-tagged FGFR wild type and activating mutants in Ishikawa cells. Spinning disk confocal microscopy time-lapse images of Ishikawa cells stably expressing eGFP-tagged FGFR wild type (left panel), or activating mutants; N550K (middle panel), Y376C (right panel). Images were acquired every 2 seconds for 1 minute. The video plays at 10 frames  $s^{-1}$  and is thus accelerated 20 times.

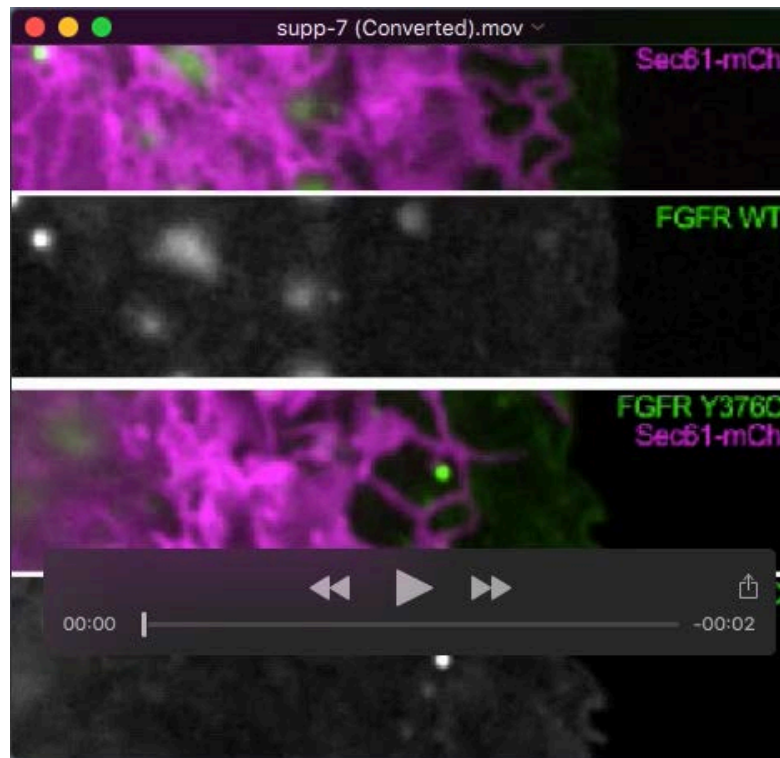


**Supplemental Movie 2** Proliferation dynamics of Ishikawa cells expressing FGFR wild-type or activating mutants. Bright field live-cell images of Ishikawa cells stably expressing eGFP alone (empty vector), WT, N550k or Y376C FGFR2b (left to right). Cells were grown in either heparin alone (top row) or heparin plus FGF10 (bottom row) in 2% serum for 6 days. Images were acquired every 2 hours for 6 days. The video plays at 10 frames s<sup>-1</sup> and is thus accelerated 518400 times.

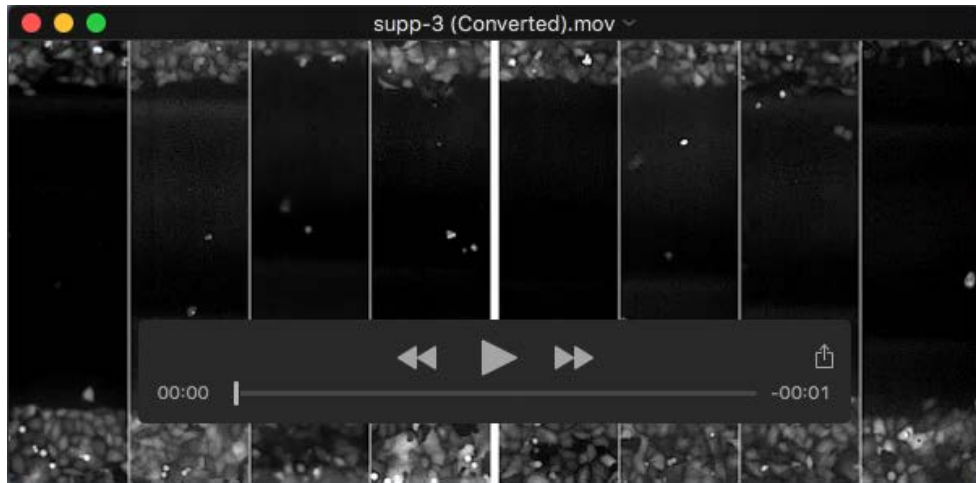




**Supplemental Movie 3** Dynamics of eGFP-tagged FGFR wild type and the activating mutant N550K intracellular vesicles in mCherry- Rab6a (Golgi) expressing Ishikawa cells. Spinning disc confocal microscopy time-lapse sequence cells co-expressing either, top panel: FGFR-WT- eGFP (green) and Rab6a-mCherry (magenta) or bottom panel: FGFR-N550K- eGFP (green) and mCherry-Rab6a (magenta). eGFP vesicles are highly dynamic in both WT and N550K and move independently of Golgi structures (mCherry-Rab6a). Images were acquired every 1 second for 2 minutes. The video plays at 10 frames s<sup>-1</sup> and is thus accelerated 10 times.



**Supplemental Movie 4** Dynamics of eGFP-tagged FGFR wild type and the activating mutant Y376C intracellular vesicles in Sec61-mCherry (ER) expressing Ishikawa cells. Spinning disc confocal microscopy time-lapse sequence cells co-expressing either, top panel: FGFR-WT- eGFP (green) and Sec-61-mCherry (magenta) and corresponding grey scale image below or bottom panel: FGFR-Y376C- eGFP (green) and Sec-61-mCherry (magenta) and corresponding grey scale image below. eGFP vesicles are highly dynamic in both WT and Y376C and move independently of ER structures (Sec61-mCherry). Images were acquired every 1 second for 1 minute. The video plays at 10 frames s<sup>-1</sup> and is thus accelerated 10 times.

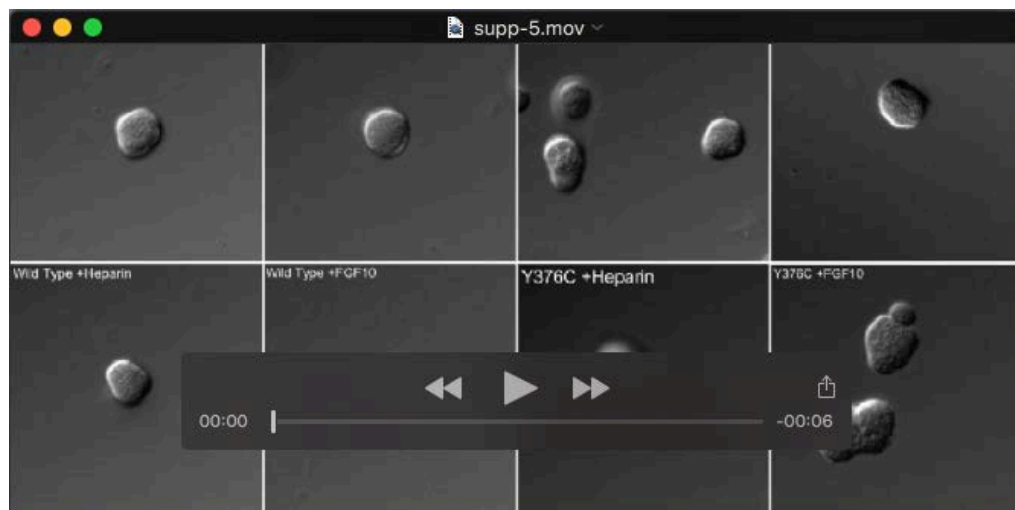


**Supplemental Movie 5** Wound closure dynamics of Ishikawa cells expressing FGFR wild-type or activating mutants. Ishikawa cells stably expressing eGFP alone (empty vector), WT, N550k or Y376C FGFR were transduced with mCherry to create a high contrast images for cell tracking by widefield epifluorescence imaging (Incucyte ZOOM®). Left four panels: cells stimulated with Heparin (5  $\mu\text{g/ml}$ ) (control). Right four panels: cell stimulated with FGF10 (50  $\mu\text{g/ml}$ ) in the presence of Heparin (5  $\mu\text{g/ml}$ ). Images were acquired every 2 hours for 24 hours. The video plays back at 10 frames  $\text{s}^{-1}$  and is thus accelerated 72000 times.



**Supplemental Movie 6** Actin dynamics in migrating Ishikawa cells expressing eGFP-tagged FGFR wild type or the activating mutant N550K. Spinning disc confocal microscopy time-lapse sequence of Ishikawa cells co-expressing eGFP-tagged receptor (magenta) with the filamentous actin reporter LifeAct-mCherry (black). Images were acquired every 3 minutes for 3 hours. The video plays back at 10 frames s<sup>-1</sup> and is thus accelerated 1800 times.





**Supplemental Movie 7** Dynamics of endometrial acinar morphogenesis and invasive migration in Ishikawa cells expressing FGFR wild-type or activating mutations. Differential Interference Contrast time-lapse images of Ishikawa acini formed from cells stably expressing eGFP alone (empty vector, upper left panels), eGFP-tagged FGFR wild type (left bottom panels), or activating mutants; N550K (upper right panels), Y376C (lower right panels). Acini were grown in growth factor reduced Matrigel™ overlay assay for 3 days prior to stimulation with either heparin alone or heparin plus FGF10 in 2% serum. Images were acquired every hour for 77 hours. The video plays back at 12 frames s<sup>-1</sup> and is thus accelerated 43200 times.